

Empirical and molecular modeling study of the pyridinium species RHPP⁺, an abundant and potentially neurotoxic metabolite of haloperidol

2 PERKIN

Frédéric Ooms,^{a*} Sébastien Delvosal,^a Johan Wouters,^a François Durant,^a Gisella Dockendorf,^d Clinton Van't Land,^b Thomas Glass,^b Neal Castagnoli, Jr.,^b and Cornelis J. Van der Schyf^{b,c,d}

^a *Laboratoire de Chimie Moléculaire Structurale, Facultés Universitaires Notre-Dame de la Paix, Namur, Belgium*

^b *Department of Chemistry and the Harvey W. Peters Center for the Study of Parkinson's Disease and Disorders of the Central Nervous System, Virginia Polytechnic Institute and State University, Blacksburg, VA 24061, USA*

^c *Department of Biomedical Sciences and Pathobiology, VA-MD Regional College of Veterinary Medicine, Virginia Polytechnic Institute and State University, Blacksburg, VA 24061, USA*

^d *Department of Pharmaceutical Chemistry, Potchefstroom University for Christian Higher Education, Potchefstroom 2520, South Africa*

Received (in Cambridge, UK) 24th March 2000, Accepted 6th June 2000

Published on the Web 11th August 2000

The “reduced” haloperidol pyridinium metabolite (RHPP⁺) is found in the brain, plasma and urine of patients treated with the neuroleptic drug haloperidol (HP). RHPP⁺ is suspected to be neurotoxic through a mechanism that entails interference with the mitochondrial electron transport chain. We have studied the conformation of this flexible molecule in solution (using NMR) and in the solid state by single crystal X-ray analysis. Using the solid state structure as initial input, molecular dynamics runs indicated that the molecule preferably exists in an unfolded, rather than a folded conformation. We propose that the interaction of RHPP⁺ with complexes in the mitochondrial respiratory chain is stabilized primarily by an ionic bond involving the cationic nitrogen and secondarily by hydrogen-bond anchoring originating from the hydroxy group. A comparison with HPP⁺, the “unreduced” pyridinium metabolite of HP, suggests that this latter interaction may—among other considerations such as lipophilicity—account for differences in the *in vitro* toxicological profiles of RHPP⁺ and HPP⁺, which carries a ketone group *in lieu* of the hydroxy.

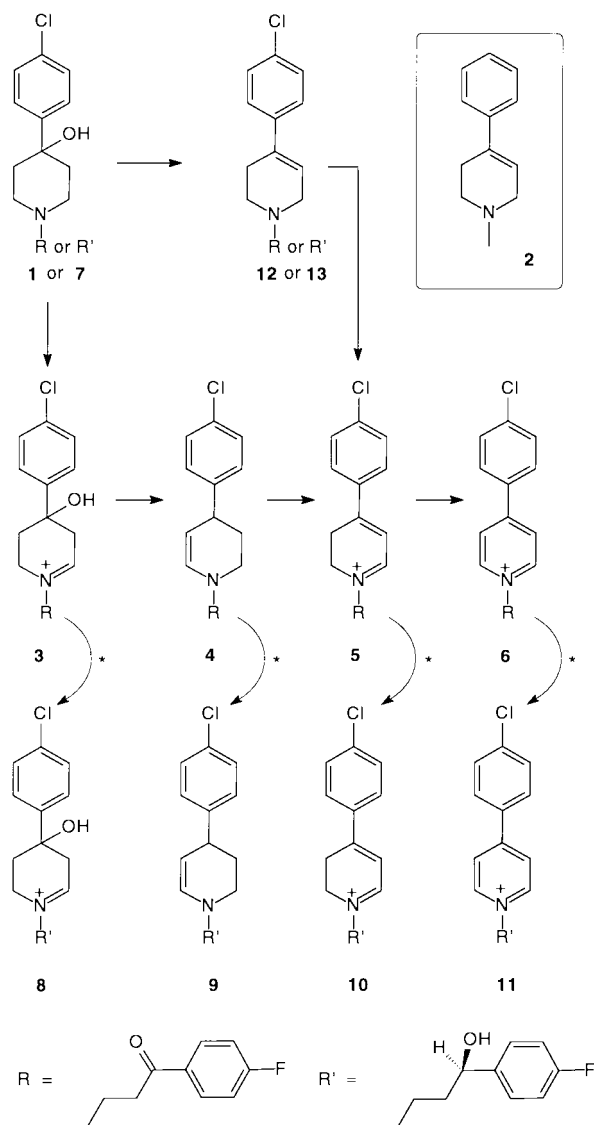
Introduction

Haloperidol, 4-[4-(4'-chlorophenyl)-4-hydroxypiperidino]-4'-fluorobutyrophenone, (HP, **1**, Scheme 1) is a potent neuroleptic agent that, like other members of this pharmacological class known as typical neuroleptics, causes severe extrapyramidal side effects including parkinsonism and a condition known as tardive dyskinesia (TD)¹ that, in many cases, is irreversible.² The irreversibility of TD suggests an underlying pathology³ that may be the result of neuroleptic treatment. HP is a 4-piperidinol derivative that resembles the parkinsonian-inducing pro-neurotoxin 1-methyl-4-phenyl-1,2,3,6-tetrahydropyridine (MPTP, **2**, Scheme 1) in that it bears an aryl group at C-4 of the azacycle.⁴ MPTP is transformed through brain monoamine oxidase B (MAO-B)⁵ and subsequent oxidation to the *N*-methyl-4-pyridinium (MPP⁺) species, its ultimate neurotoxic form.⁶ Simple dehydration of HP, a reaction which is reported to occur in microsomal incubations,⁷ gives rise to the corresponding 1,2,3,6-tetrahydropyridine derivative HPTP (**12**, Scheme 1), an even closer analog of MPTP.

Similar to MPTP, the structural features present in HP also predispose this compound to an oxidative pathway leading to pyridinium metabolites.⁸ Ring α -carbon oxidation of the piperidine derivatives (**1**, **7**) bearing a leaving group (OH) at C-4 generates the corresponding iminium metabolites **3** and **8** that, *via* the enamines **4** and **9**, will undergo spontaneous

conversion to the dihydropyridinium intermediates **5** and **10** (Scheme 1). Dihydropyridinium compounds **5** and **10** undergo spontaneous autoxidation to form the pyridinium species HPP⁺ (**6**)⁸ and RHPP⁺ (**11**).^{9,10} HP (**1**) and its principal circulating metabolite in humans, (*S*)-(-) “reduced” HP (RHP, **7**),¹¹ are both candidates for such reaction sequences (**1**→**3**→**4**→**5**→**6**, in the case of HP, and **7**→**8**→**9**→**10**→**11**, in the case of RHP). Alternatively, simple dehydration of **1** and **7** could generate the corresponding tetrahydropyridine derivatives HPTP (**12**)¹² and RHPTP (**13**) respectively which, following ring α -carbon oxidation, would yield the same dihydropyridinium intermediates **5** and **10**.¹³

The metabolic fate of HP (**1**) has been examined in rodents^{12,19} and baboons¹³ treated with either HP or HPTP (**12**) and in humans treated with HP^{9,21} employing LC-MS/MS and LC-fluorescence techniques designed to detect pyridinium metabolites. The results of the studies in rodents and baboons have established that both HP and HPTP are biotransformed to the HP pyridinium metabolite HPP⁺ (**6**), as is HP in humans. Unlike the corresponding conversion of MPTP to the neurotoxic pyridinium species MPP⁺, the oxidative biotransformation of HP to HPP⁺ is not mediated by MAO-B.⁸ Neither HP nor HPTP are substrates for MAO-B, although both are biotransformed to the pyridinium product by rat and human liver microsomal preparations,⁸ but the conversion of HPTP to HPP⁺, presumably *via* the dihydropyridinium intermediate **5**, is catalyzed by MAO-A.²² Recent findings^{10,14-16} have led to the



Scheme 1 Chemical structures of compounds discussed in the text, also illustrating the proposed catalytic pathway for the cytochrome P450-catalyzed (P450 3A4) oxidation of HP (1) to HPP⁺ (6) and RHPP⁺ (11). In the human,^{11,17,18} and primate,¹³ but not rat^{19,20} conversion of the keto compounds (1, 3–6) to their hydroxy counterparts (7–11) may occur at any of the pathways designated * through catalyses by ketone reductases.¹¹

identification of cytochrome P450 3A4 as the principal catalyst responsible for these oxidative conversions.

The related HP pyridinium metabolite, 4-(4-chlorophenyl)-1-[4-(4-fluorophenyl)-4-hydroxy]butylpyridinium RHPP⁺ (11), in which the butyrylphenone carbonyl group of HPP⁺ is reduced to the corresponding alcohol, has also been detected in the human.^{9,10,21} Both HP and HPTP are also biotransformed in mice^{4,12} and baboons¹³ to RHPP⁺. RHPP⁺ is likely to be primarily derived from RHP (7), the major circulating metabolite of HP that is generated by NADPH-dependent ketone reductase,^{4,11} and from HPP⁺, also *via* ketone reductases.¹⁰ In the human¹⁸ and the primate,¹³ RHPP⁺ has been found in more abundant quantities in plasma and urine than HPP⁺.

There is reasonable evidence to suspect that HPP⁺ and possibly RHPP⁺, when formed in the brain,¹⁷ could cause neuronal injury that may be involved in irreversible TD. However, evidence to support a neuroleptic-induced pathological brain lesion in humans³ and animals^{3,23–27} is limited. Pyridinium species such as HPP⁺²⁸ and RHPP⁺ are potent inhibitors at Complex I (NADH dehydrogenase)^{29,30} and IV

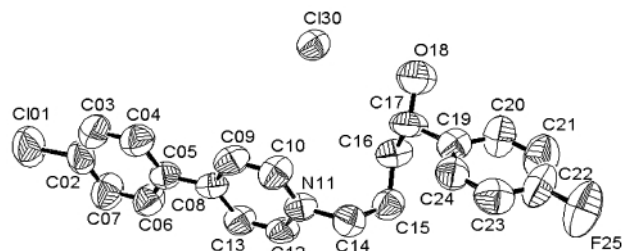


Fig. 1 Structure and solid-state conformation of RHPP⁺. Non-H atoms are represented by displacement ellipsoids at the 50% probability level.

(unpublished data) of the mitochondrial electron transport chain and found *in vitro* to be neurotoxic.³¹

In an effort to correlate the structure of pyridinium compounds with inhibition of mitochondrial respiration, Nicklas and co-workers^{32–34} studied a series of 4'-alkylated analogs of MPP⁺. The potencies of these compounds agreed with their ability to partition between octan-1-ol and water. In mitochondria, increased hydrophobicity resulted in increased inhibition of Complex I. Furthermore, the pyridinium charge was found to play a major role in explaining the inhibitory mechanism of the pyridiniums because the potencies of these species were found to be much greater than would be predicted based solely on hydrophobicity.^{34–36} It has recently been demonstrated that flexible bioactive molecules may adopt conformations in the solid state which are usually held in aqueous medium only through the process of hydrophobic collapse.³⁷ Due to their flexibility and the possibility of undergoing hydrophobically induced folding,³⁸ the pyridinium metabolites of HP warrant study of their conformations in the solid state and in solution, in an effort to better understand their interactions with electron transfer complexes in the mitochondrial respiratory chain. We have recently reported on the molecular conformation of HPP⁺.³⁹ Our current report documents the conformational properties of the even more abundant HP pyridinium metabolite RHPP⁺ as determined by single crystal X-ray diffraction studies,¹ ¹H NMR and 2D-NOESY measurements and computational chemistry (high temperature molecular dynamics) with a view to propose a model for structural properties that may dictate the interaction of RHPP⁺ with electron transfer complexes in the mitochondrial respiratory chain.

Results

Description of the X-ray structure

Fig. 1 shows a view of the molecular conformation of RHPP⁺. The lattice constants are listed with other relevant crystal data in Table 1. Table 2 lists the main torsion angles. The butyryl chain adopts a *g⁺g⁺g⁺g⁺* conformation. The chlorophenyl ring is coplanar with the pyridinium ring (Table 2). This coplanarity may be explained in terms of packing constraints forcing both rings to orient in the same plane, allowing optimal stacking of the molecules in the crystal. This phenomenon has also been observed in the X-ray structure of HPP⁺.³⁹ The biphenyl fragments tended also to crystallize in an approximately planar geometry when there are no substituents in the *ortho* position,⁴⁰ despite the fact that the inter-ring dihedral angle in the vapor phase is reported to be 44°. Analysis of the forces responsible for crystal cohesion also may suggest potential anchoring points of the molecule under conditions representing biological interactions. Our analysis shows that the molecules in the crystal lattice are linked to each other through H-bonds with the chlorine ions Cl30, the values of which are reported in Table 3.

CSD statistical analysis of the hydrogen bond properties of the benzyl ketone and benzyl alcohol model systems

The characterization of the orientation of H-bonds in biological systems is important in understanding biochemical interactions. Recent surveys have been done on the three-dimensional H-bond geometry by analysis of the Cambridge Structural Database (CSD).^{42–44} Ketone and hydroxy groups present respectively in HPP⁺ and RHPP⁺ could play an important role in interactions with biological macromolecules. We analyzed benzyl ketone and benzyl alcohol model systems, as similar systems were not included in the earlier published surveys.

Table 1 Crystallographic data, data collection and refinement parameters for RHPP⁺Cl^{-a}

Crystallographic data	
Chemical formula	(C ₂₁ H ₂₁ NOCIF) ⁺ Cl ⁻
Formula weight	357.86
Crystal system	Monoclinic
Space group	P2(1)/c
<i>a, b, c</i> /Å	13.806(3), 14.710(3), 9.618(2)
alpha, beta, gamma/°	90, 92.77(3), 90
<i>V</i> /Å ³	1951.0(7)
<i>Z</i>	4
μ (Cu-K α)/mm ⁻¹	3.15
Data collection	
Temperature/K	293(2)
Reflections collected	3409
Independent reflections	2820
<i>R</i> (int)	0.066
Observed data [<i>I</i> > 2 σ (<i>I</i>)]	1273
Refinement	
Final <i>R</i> 1 [<i>I</i> > 2 σ (<i>I</i>)]	0.0957
Final <i>R</i> 1 (all merged data)	0.1905
<i>wR</i> 2 ^b	0.2537

^a Atomic scattering factors from International Tables Vol. C, Tables 4.2.6.8 and 6.1.1.4. ^b *w* = calc *w* = 1/[$\sigma^2(F_o^2) + (0.218P)^2 + 0.0000P$] where $P = (F_o^2 + 2Fc^2)/3$.

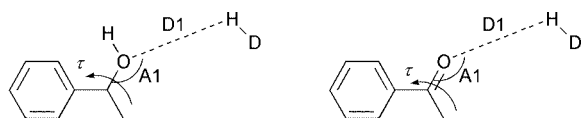


Fig. 2 Geometrical descriptor used for the analyses of the hydrogen bond. D1 represents the H-bond length, A1 the H-bond angle and τ the torsion angle.

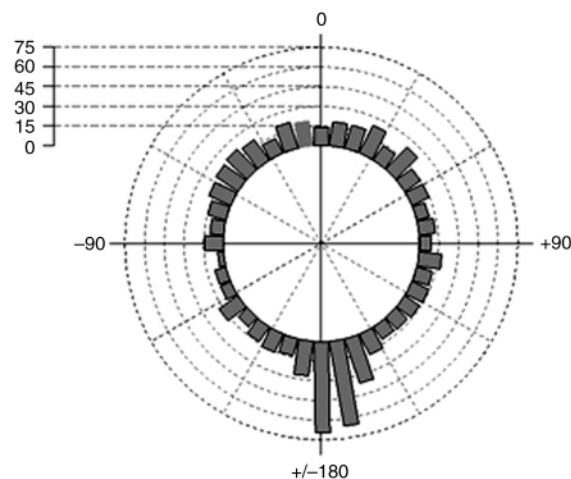
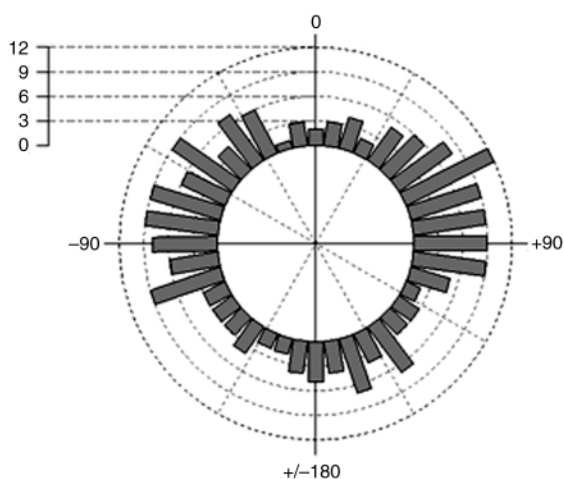


Fig. 3 Polar scattergram of the directionality parameter, τ , for the benzyl alcohol model (left). Polar scattergram of the directionality parameter, τ , for the benzyl ketone model (right).

The CSD search led to the identification of 750 H-bond interactions for the sp² oxygen and 216 H-bonds for the sp³ oxygen. Three descriptors (Fig. 2) were considered in order to characterize the H-bond geometry by monitoring the torsion angle, τ . The greatest probability of forming an H-bond with the benzyl ketone system corresponded to a τ angle approaching 180° (*i.e.* coplanar relative to the phenyl ring) while for the benzyl alcohol system this angle is closer to 90°, *i.e.* perpendicular relative to the phenyl ring (Fig. 3).

Nuclear magnetic resonance

(a) ¹H NMR measurements. We examined the conformational properties of RHPP⁺ in solution using NMR spectroscopy with CD₃OD as solvent. The atomic numbering of RHPP⁺ is shown in Fig. 4. The low-field (7.2–8.2 ppm) region of the ¹H spectrum contains two well-resolved symmetrical doublets centered at 7.81 and 8.17 ppm, a multiplet at 7.53 ppm and a triplet at 7.21 ppm. The signals at 7.21 and 7.53 ppm are part of the AA'BB'X system associated with *p*-fluorobenzene compounds. The multiplet at 7.53 ppm is assigned to the H20 (= H24) resonance, which is coupled to H21 (= H23) ($J_{HH} = 8.6$ Hz), H24, and to fluorine. The apparent triplet at 7.21 ppm is assigned to the H21 proton coupled to H20 and to fluorine with similar coupling constants ($J_{HH} = 8.8$ Hz) and to H23. These patterns are also seen—virtually identical in form—in the ¹H NMR spectrum of *p*-fluoroacetophenone, whereas *p*-chloroacetophenone has a single symmetrical AB multiplet.⁴⁵ The symmetrical AB (simplified AA'BB') pattern centered at 8.00 ppm consists of two doublets centered at 7.81 (H7 = H3) and 8.17 ppm (H6 = H4) with $J_{HH}(J_{AB}) = 8.7$ and 8.6 Hz respectively.

Table 2 Main torsion angles (°) of RHPP⁺ with esd's in parentheses

N11–C14–C15–C16	64.9(10)
C14–C15–C16–C17	61.9(11)
C15–C16–C17–C19	54.6(12)
C16–C17–C19–C24	–103.1(10)
C04–C05–C08–C09	–178.4(8)
C04–C05–C08–C13	–179.5(8)

Table 3 Hydrogen-bonding geometry (Å, °)

D–H...A	<i>d</i> (D–H)	<i>d</i> (H...A)	D–H...A	<i>d</i> (D...A)
O18–H18...Cl30	0.820	2.346	160.04	3.131(6)

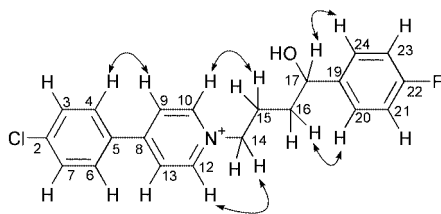


Fig. 4 Atomic numbering of RHPP⁺ used in ¹H-NMR interpretation and through-space interactions observed by NOESY as indicated by arrows.

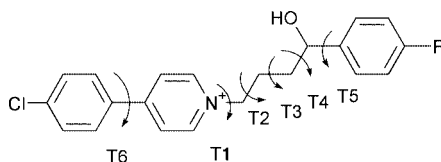


Fig. 5 Torsion angles designation of the planar structure of RHPP⁺ used in the MD analysis.

The methylene protons are located at 1.94 (H16), 2.28 (H15), 4.83 (H14) and 4.89 (H17) ppm as two multiplets and two triplets, with $J_{\text{HH}} = 7.3, 7.3, 7.48$ and 6.33 Hz for each signal. The pyridinium ring protons are centered at 8.56 (H13, H9) and 9.14 (H12, H10) ppm as doublets. In CD₃OD J_{HH} for H9 is 7.0 Hz and 6.7 Hz for H10. Identical patterns are seen in the proton spectrum of 1-heptyl-4-(4-pyridyl)pyridinium bromide for the pyridinium ring protons.⁴⁶

(b) 2D-NOESY measurements. Through-space interactions in RHPP⁺ were established by 2D-NOESY measurements. This proved particularly helpful where the results of a typical 2D-NOESY experiment not only verified earlier 1D assignments, but also provided important information about the conformation of RHPP⁺ in solution.

All the through-space interactions confirmed the connectivity assignments made with H,H-COSY. Of considerable interest in the conformational analyses were the 2D-NOESY cross peaks shown for the H17–H20(= H24), H16(a,b)–H20(= H24), H14(a,b)–H10(= H12), H15(a,b)–H10(= H12) and H9(= H13)–H4(= H6). The observed through-space interactions for RHPP⁺ are shown in Fig. 4.

Conformational analysis by molecular dynamics (MD)

The solid state structure of (*S*)-RHPP⁺ served as the starting geometry for molecular modeling studies in which the conformational space of the molecule was explored by MD. During each MD simulation 20 conformers were saved after subsequent minimizations. These simulations were repeated 10 times, using different starting geometries for RHPP⁺ to generate a total of 200 conformations. This methodology has already been used and validated with HPP⁺.³⁹

All the energies of the obtained conformers occurred within a range of 3 kcal mol⁻¹. The torsion angles were defined as illustrated in Fig. 5. The most frequently observed torsion angle for T1 was found to be approximately 90° (Fig. 6). This torsion angle was also observed in the X-ray structures of RHPP⁺ (Table 2) and HPP⁺.³⁹ The most frequent values for torsion angle T5 were found to occur at 60° and 130° (Fig. 7). These values also approached those observed for the same angle in the X-ray structure (Table 2).

A cluster analysis was then performed with the Analysis module of MSI/Biosym.⁴⁷ Among the 200 conformers generated by MD, 57 families were defined on the basis of root mean square (RMS) fit on the heavy atoms of RHPP⁺ (RMS < 0.75 Å). From these data it is clear that, as expected, RHPP⁺ behaves with substantial flexibility.

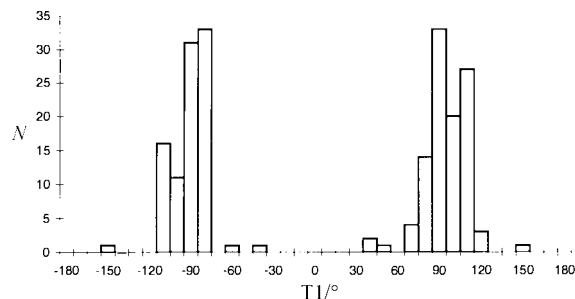


Fig. 6 Frequency of observation of T1 in the MD simulations.

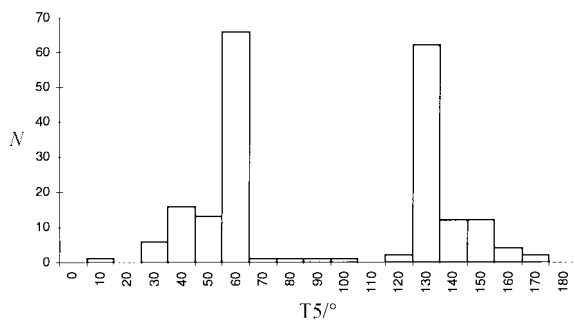


Fig. 7 Frequency of observation of T5 in the MD simulations.

From the 57 families defined, the frequency of observation of the distance between the centroids of the fluorophenyl and the pyridinium rings was studied. This analysis suggested that there are 2 types of possible conformations, *i.e.* folded (distance < 5 Å), and unfolded (distance > 6.5 Å). The ratio of folded to unfolded structures is approximately 1:9. For the folded structures, it was noticeable that the interproton distances between the fluorophenyl and pyridinium rings were less than 5 Å. The unfolded conformation is also the one observed in the solid state (Fig. 1).

Discussion

Our earlier study³⁹ on the conformational distribution of HPP⁺, combined with recent studies performed on isoquinoline derivatives, another family of inhibitors at complexes in the mitochondrial electron transport chain,^{48–51} led to the proposition of a hypothetical binding model for haloperidol pyridinium compounds.³⁹ We propose that HPP⁺ might act by interacting with mitochondrial respiratory complex(es) through a primary ionic bond involving the cationic nitrogen reinforced by stabilization of the lateral chain *via* H-bonding. Assuming this hypothesis, the folded structures of HPP⁺ and RHPP⁺ were discarded because the cationic charge on the nitrogen was conformationally inaccessible in these forms. This hypothesis also is supported by the NMR analyses performed on both HPP⁺³⁹ and RHPP⁺. In solution, no NOESY cross peaks were observed between the protons of the fluorophenyl and pyridinium rings (Fig. 4). The ¹H-NMR chemical shifts also suggest an unfolded structure because of the lack of any upfield shifts that may be indicative of ring current shielding. Virtually identical patterns are seen in the ¹H-NMR spectrum of *p*-fluoroacetophenone⁴⁵ and 1-heptyl-4-(4-pyridyl)pyridinium bromide⁴⁶ for the pyridinium ring protons. The similarities in the patterns of the ¹H-NMR spectrum of RHPP⁺ with the spectra of these compounds suggest that no intramolecular interactions exist between the phenyl rings present in RHPP⁺.

The pyridinium ring common to both HPP⁺ and RHPP⁺ was used to superimpose the unfolded conformations of these compounds. This superimposition shows that the spaces explored by the fluorophenyl ring of HPP⁺ and RHPP⁺ are not equivalent as a consequence of the presence of carbonyl *versus* hydroxy in the butyryl chain. However, if the positions of the

oxygen are considered, only two common zones for HPP⁺ and RHPP⁺ may be circumscribed (Fig. 8). Based on this latter superimposition, the H-bond could act as a common anchoring point for these two compounds. Moreover, this H bonding interaction could explain the greater *in vitro* toxicity²⁸ of these compounds *versus* the MPP⁺-like compounds that lack this supplementary element in the pharmacophore. Analysis of this superimposition allowed identification of those HPP⁺ and RHPP⁺ conformers whose oxygen moieties occupy exactly the same space. According to these criteria, four families of conformers were retained (two for HPP⁺ and two for RHPP⁺). These families are symmetry-related to one another, therefore leaving only one conformation per compound (Table 4). Superimposition of the region in which H-bond formation is most likely to occur shows that the H-bond has the same directionality for the two fragments (Fig. 9). Based on this study, the difference in *in vitro* toxicity to mitochondrial complexes of HPP⁺ and RHPP⁺ (unpublished data) may also be explained. Indeed, in this model, the fluorophenyl moiety of the two compounds do not share the same conformational space, leading to a situation where this moiety could induce steric hindrance or be subject to lower stabilization within a hydrophobic pocket in the case of HPP⁺ (Fig. 9).

Table 4 Main geometrical features of the proposed bioactive conformations. Torsion angles (°) T1–T5 defined in Fig. 5.

	T1	T2	T3	T4	T5
HPP ⁺	79.4	64.1	-176.7	109.3	-178.9
RHPP ⁺	77.2	66.4	-179.4	-64.4	92.6

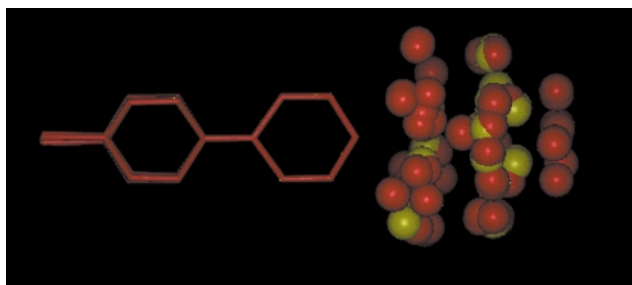
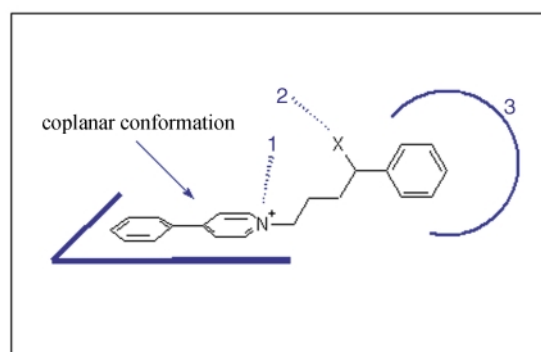


Fig. 8 Superimposition of HPP⁺ (yellow) and RHPP⁺ (red). For clarity only the oxygen of the hydroxy group present on the side chain linked to the pyridinium ring is shown.



- (1) Stabilization through an ionic bond involving the cationic nitrogen
- (2) H-bond interaction with a donating group (X)
- (3) Steric hindrance or lower stabilization in a hydrophobic pocket (see text)

Conclusion

In this study we propose a model for the bioactive conformations of HPP⁺ and RHPP⁺, both putative neurotoxic metabolites of HP. The proposal is based on the conformation of HPP⁺, reported earlier,³⁹ and RHPP⁺, reported in this study and obtained by X-ray crystallography, NMR and molecular dynamics methods. This model was found to agree with the favored binding mode of isoquinoline derivatives^{48–51} by stabilization through an ionic bond involving the cationic nitrogen. Both in HPP⁺ and RHPP⁺ an additional H-bond, interacting with the oxygen of the side chain, can also be proposed. Steric interactions or hydrophobic stabilization induced by the fluorophenyl moiety may explain differences in toxicity between these two compounds. We are currently investigating further the inhibitory properties of HPP⁺ and RHPP⁺ in leukocyte models of mitochondrial respiration. We also plan to synthesize analogs of these pyridiniums that are designed to explore the proposed features of their site of interaction with mitochondrial complexes with a view to shedding further light on the toxicology of these species.

Experimental

Crystallography

The chloride salt of RHPP⁺ was synthesized as described elsewhere.¹² Crystals are hard to grow. One crystal suitable for X-ray analysis was obtained by slow evaporation of a saturated chloroform–methanol solution. All diffraction measurements were performed at 293 K and collected with an Enraf-Nonius CAD-4 diffractometer equipped with a copper anode. The lattice constants are listed with other relevant crystal data in Table 1.† A complete data set was collected to a maximum theta limit of 62° resulting in a total of 3409 reflections. Due to crystal degradation, no data could be collected (ψ -scan) to correct for absorption effects, neither could the crystal be precisely measured. The data (2820 unique reflections) were corrected for Lorentz and polarization effects using the in-house program NONIUS93.⁵² The structure was solved and refined using the SHELXL 97 program.⁵³ Hydrogen atoms were calculated at their standard positions and treated in a riding model. No absorption correction could be applied to the data.

† CCDC reference number 188/254. See <http://www.rsc.org/suppdata/p2/b0/b002357o> for crystallographic files in .cif format.

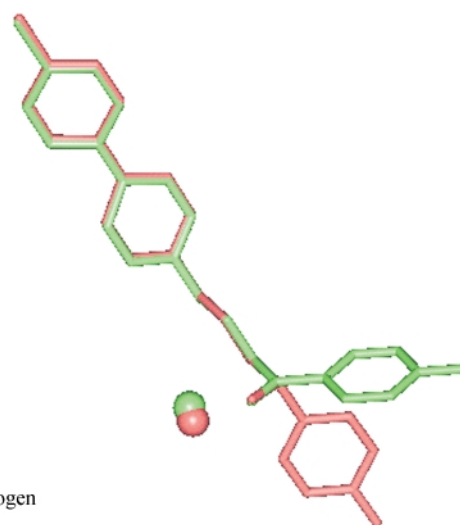


Fig. 9 Proposed model of the bioactive conformations of HPP⁺ and RHPP⁺ (right) and schematic representation of the proposed binding mode of those compounds (left).

Statistical analysis of the hydrogen bond properties of benzyl ketone and benzyl alcohol model systems

The Cambridge Structural Database (CSD, Version 5.12, October 1996) was used in this work.⁵⁴ Searches for bonded substructures and short non-covalent intramolecular contacts were carried out using the program QUEST3D (Cambridge Structural Database, 1994). Data display and analyses were performed with VISTA (Cambridge Structural Database, 1995). The first stage of the search identified close intermolecular contacts, with D1 values less than 3.2 Å and A1 values of more than 90° (Fig. 2). The fragments also had to satisfy the following search criteria: (a) organic compounds, (b) error-free coordinate sets, (c) no disorder, (d) not polymeric and (e) *R* less than 0.10. These criteria reduced the number of structures to about 48,000. All H atoms involved in non-bonded contact searches were placed in neutron-normalized positions.

Conformational search by molecular dynamics simulations

All calculations were carried out using the second generation forcefield CFF91 of Maple, *et al.*^{55,56} The Discover 95.0 simulation program within Biosym/MSI's InsightII,⁵⁷ was used to perform the calculations. Molecular dynamics (MD) were carried out using a relative permittivity (RP) of 32.63 to roughly simulate the conditions under which the NMR data were obtained.

For the first dynamics run the X-ray structure was used as the starting conformation and subjected to a 5 ps simulation at 600 K, after which the coordinates were stored and velocities randomized in order to generate a new structure for the next 5 ps simulation. The procedure was repeated twenty times in order to generate twenty structures for a total run of 100 ps. The twenty conformers generated were submitted to an annealing protocol in which the temperature was gradually reduced to 300 K during a 15 ps MD run and then minimized by steepest descent and conjugate gradient to a final root mean square (RMS) gradient of less than 0.001 kcal mol⁻¹. Ten subsequent simulations were performed using as starting conformations other second minimum energy conformations generated in the first run. All the conformations generated in this manner were grouped into families of similar structure using the Analysis module of Biosym/MSI.⁴⁷ This procedure has already been used and validated in a previous study of HPP⁺.³⁹ All calculations were performed on the IBM RS-6000 computer system of the Scientific Computing Facility Center of the University of Namur.

Nuclear magnetic resonance

(a) ¹H NMR measurements. ¹H NMR spectra were recorded on a Varian Unity 400 MHz NMR spectrometer in CD₃OD (Aldrich, atom 99.9% ²H enriched) observing ¹H at 399.95 MHz. All samples were prepared in 5 mm tubes (Wilma Glass Company, 528-PP grade) and analyzed at 298 K. The samples were purged with nitrogen gas and the tubes sealed under high vacuum prior to spectral acquisition. Spectra were internally referenced to the solvent resonance. The ¹H spectra were collected into 37K data sets and zero filled to 64K over a spectral width of 5 kHz using a 25° pulse.

(b) 2D-NOESY measurements. The homonuclear ¹H-¹H dipolar correlated 2D spectra were obtained using the NOESY pulse sequence. The spectral widths were typically *F*₂ = 3000 Hz. The spectra were collected as 1024 × 1024 blocks of data and were processed by sinusoidal (shifted by 1/3) multiplication in each dimension followed by symmetrization of the final data matrix. Other parameters were as follows: number of increments in *t*₁, 256 scans, 8 relaxation delays of 6 s and a mixing time of 600 ms.

Acknowledgements

The authors acknowledge IBM Belgium and the Facultes Notre Dame de la Paix for the use of the Namur Scientific Computing Facilities. The study was supported by the Peters Center for the Study of Parkinson's Disease and Disorders of the Central Nervous System, Virginia Tech, Blacksburg, VA.

References

- 1 J. Gerlach and D. E. Casey, *Acta Psychiatr. Scand.*, 1988, **77**, 369.
- 2 D. E. Casey, U. J. Povlsen, B. Meidahl and J. Gerlach, *Psychopharmacol. Bull.*, 1985, **22**, 250.
- 3 K. Jellinger, in *Neurotoxicology*, ed. H. Roizin, H. Shiraki and N. Grevic, Raven Press, New York, 1977, pp. 25–42; G. M. Halliday, S. M. Pond, H. Cartwright, D. E. McRitchie, N. Castagnoli, Jr. and C. J. Van der Schyf, *Exp. Neurol.*, 1999, **158**, 155.
- 4 C. J. Van der Schyf, E. Usuki, S. M. Pond and N. Castagnoli, Jr., in *Highly Selective Neurotoxins: Basic and Clinical Applications*, ed. R. M. Kostrzewa, Humana Press, Totowa, New Jersey, 1998, pp. 195–210; E. Usuki, C. J. Van der Schyf and N. Castagnoli, Jr., *Drug Metab. Rev.*, 1998, **30**, 809.
- 5 N. Castagnoli, Jr., K. Chiba and A. J. Trevor, *Life Sci.*, 1985, **36**, 225.
- 6 K. Chiba, A. Trevor and N. Castagnoli, Jr., *Biochem. Biophys. Res. Commun.*, 1985, **128**, 1228.
- 7 J. Fang and J. W. Gorrod, *Toxicol. Lett.*, 1991, **59**, 117.
- 8 B. Subramanyam, T. Woolf and N. Castagnoli, Jr., *Chem. Res. Toxicol.*, 1991, **4**, 123.
- 9 D. W. Eyles, H. R. McLennan, A. Jones, J. J. McGrath, T. J. Stedman and S. M. Pond, *Clin. Pharmacol. Ther.*, 1994, **56**, 512.
- 10 D. W. Eyles, J. J. McGrath and S. M. Pond, *Psychopharmacology*, 1996, **125**, 214.
- 11 D. W. Eyles and S. M. Pond, *Biochem. Pharmacol.*, 1992, **44**, 867.
- 12 C. J. Van der Schyf, K. Castagnoli, E. Usuki, H. G. Fouda, J. M. Rimoldi and N. Castagnoli, Jr., *Chem. Res. Toxicol.*, 1994, **7**, 281.
- 13 K. M. Avent, E. Usuki, D. W. Eyles, R. Keeve, C. J. Van der Schyf, N. Castagnoli, Jr. and S. M. Pond, *Life Sci.*, 1996, **59**, 1473.
- 14 K. Igarashi, F. Kasuya, M. Fukui, E. Usuki and N. Castagnoli, Jr., *Life Sci.*, 1995, **57**, 2439.
- 15 E. Usuki, R. Pearce, A. Parkinson and N. Castagnoli, Jr., *Chem. Res. Toxicol.*, 1996, **9**, 800.
- 16 J. Fang, G. B. Baker, P. H. Silverstone and R. T. Coutts, *Cell. Molec. Neurobiol.*, 1997, **17**, 227.
- 17 D. W. Eyles, K. M. Avent, T. J. Stedman and S. M. Pond, *Life Sci.*, 1997, **60**, 529.
- 18 K. M. Avent, R. R. Riker, G. L. Fraser, C. J. Van der Schyf, E. Usuki and S. M. Pond, *Life Sci.*, 1997, **61**, 2383.
- 19 B. Subramanyam, H. Rollema, T. Woolf and N. Castagnoli, Jr., *Biochem. Biophys. Res. Commun.*, 1990, **166**, 238.
- 20 N. Castagnoli, Jr., J. M. Rimoldi, J. Bloomquist and K. P. Castagnoli, *Chem. Res. Toxicol.*, 1997, **10**, 924.
- 21 B. Subramanyam, S. M. Pond, D. W. Eyles, H. A. Whiteford, H. G. Fouda and N. Castagnoli, Jr., *Biochem. Biophys. Res. Commun.*, 1991, **181**, 573.
- 22 E. Usuki, in *Studies on the metabolic bioactivation of haloperidol (HP) and its tetrahydropyridine dehydration product*, PhD Thesis, Virginia Polytechnic Institute and State University, Blacksburg, VA, 1996, pp. 53–60.
- 23 C. K. Meshul and D. E. Casey, *Brain Res.*, 1989, **489**, 338.
- 24 C. K. Meshul, A. Janowsky, D. E. Casey, R. K. Stallbaumer and B. Taylor, *Psychopharmacology (Berlin)*, 1992, **106**, 45.
- 25 C. K. Meshul, R. K. Stallbaumer, B. Taylor and A. Janowsky, *Brain Res.*, 1994, **648**, 181.
- 26 C. K. Meshul, R. K. Stallbaumer and C. Allen, *Psychopharmacology (Berlin)*, 1995, **121**, 461.
- 27 R. C. Roberts, L. A. Gaither, X.-M. Gao, S. M. Kashyap and C. A. Tammenga, *Synapse*, 1995, **20**, 234.
- 28 H. Rollema, M. Skolnik, J. D'Engelbronner, K. Igarashi, E. Usuki and N. Castagnoli, Jr., *J. Pharmacol. Exp. Ther.*, 1994, **268**, 380.
- 29 C. Burckhart, J. P. Kelly, Y. H. Lim, C. M. Filley and W. D. Parker, *Ann. Neurol.*, 1993, **33**, 512; J. A. Prince, M. S. Yassin and L. Orelan, *J. Pharmacol. Exp. Ther.*, 1997, **280**, 261.
- 30 L. J. Mienie, J. J. Bergh, E. Van Staden, S. J. Steyn, S. M. Pond, N. Castagnoli, Jr. and C. J. Van der Schyf, *Life Sci.*, 1997, **61**, 265;

- L. J. Mienie, J. J. Bergh, J. R. Bloomquist, N. Castagnoli, Jr., S. J. Steyn and C. J. Van der Schyf, *Life Sci.*, 1999, **65**, 535.
- 31 J. Bloomquist, E. King, A. Wright, C. Mytilineou, K. Kimura, K. Castagnoli and N. Castagnoli, Jr., *J. Pharmacol. Exp. Ther.*, 1994, **270**, 822; N. Castagnoli, Jr., K. Castagnoli, C. J. Van der Schyf, E. Usuki, K. Igarashi, S. J. Steyn and R. R. Riker, *Pol. J. Pharmacol.*, 1999, **51**, 31.
- 32 W. J. Nicklas, M. S. Saporito, A. Basma, H. M. Geller and R. E. Heikkila, *Ann. N. Y. Acad. Sci.*, 1992, **648**, 28.
- 33 M. S. Saporito, R. E. Heikkila, S. K. Youngster, W. J. Nicklas and H. M. Geller, *J. Pharmacol. Exp. Ther.*, 1992, **260**, 1400.
- 34 M. R. Gluck, S. K. Youngster, R. R. Ramsay, T. P. Singer and W. J. Nicklas, *J. Neurochem.*, 1994, **63**, 655.
- 35 R. R. Ramsay, J. I. Salach and T. P. Singer, *Biochem. Biophys. Res. Commun.*, 1986, **134**, 743.
- 36 R. R. Ramsay, J. I. Salach, J. Dadgar and T. P. Singer, *Biochem. Biophys. Res. Commun.*, 1986, **135**, 269.
- 37 Q. Gao and W. L. Parker, *Tetrahedron*, 1996, **52**, 2291.
- 38 L. F. Newcomb, T. S. Haque and S. H. Gellman, *J. Am. Chem. Soc.*, 1995, **117**, 6509.
- 39 F. Ooms, J. Wouters, F. Durant, N. Castagnoli, Jr., C. Van't Land, G. Dockendorf, T. Glass and C. J. Van der Schyf, *J. Chem. Soc., Perkin Trans. 2*, 1997, 2627.
- 40 C. P. Brock and R. P. Minton, *J. Am. Chem. Soc.*, 1989, **111**, 4586.
- 41 A. Almenningen, O. Bastiansen, L. Fernholt, B. N. Cyvin, S. J. Cyvin and S. Sandal, *J. Mol. Struct.*, 1985, **128**, 59.
- 42 B. Pirard, G. Baudoux and F. Durant, *Acta Crystallogr.*, 1995, **B51**, 103.
- 43 J. E. J. Mills and P. M. Dean, *J. Comput. Aided Mol. Des.*, 1996, **10**, 607.
- 44 F. H. Allen, C. M. Bird, R. S. Rowland and P. R. Raithby, *Acta Crystallogr.*, 1997, **B53**, 680.
- 45 C. J. Pouchert, *Aldrich library of NMR spectra*, Vol. 2, 2nd edn., 1993, Milwaukee WI, Aldrich Chemical Company, p. 1220.
- 46 C. J. Pouchert and J. Behnke, *Aldrich library of ¹³C and ¹H FT NMR spectra*, Vol. 3, Milwaukee WI, Aldrich Chemical Company, p. 1035.
- 47 *InsightIII User Guide 1995*, Biosym/Molecular Simulations Inc., San Diego, CA.
- 48 K. S. McNaught, U. Thull, P.-A. Carrupt, C. Altomare, S. Cellamare, A. Carotti, B. Testa, P. Jenner and C. D. Marsden, *Biochem. Pharmacol.*, 1995, **50**, 1903.
- 49 K. S. McNaught, U. Thull, P.-A. Carrupt, C. Altomare, S. Cellamare, A. Carotti, B. Testa, P. Jenner and C. D. Marsden, *Biochem. Pharmacol.*, 1996, **51**, 1503.
- 50 K. S. McNaught, U. Thull, P.-A. Carrupt, C. Altomare, S. Cellamare, A. Carotti, B. Testa, P. Jenner and C. D. Marsden, *Neurodegeneration*, 1996, **5**, 265.
- 51 K. S. McNaught, U. Thull, P.-A. Carrupt, C. Altomare, S. Cellamare, A. Carotti, B. Testa, P. Jenner and C. D. Marsden, *Neurosci. Lett.*, 1996, **206**, 37.
- 52 G. Baudoux and G. Evrard, *NONIUS93, Program for Data Reduction*, 1993.
- 53 G. M. Sheldrick and T. R. Schneider, *SHELXL: High Resolution Refinement*; ed. R. M. Sweet and C. W. J. Carter, Academic Press, Orlando, Florida, 1997, vol. 277, pp. 319–343.
- 54 F. H. Allen and O. Kennard, *Chem. Design Automat. News*, 1993, **8**, 1 and 31.
- 55 J. R. Maple, U. Dinur and A. T. Hagler, *Proc. Natl. Acad. Sci. USA*, 1985, **85**, 5350.
- 56 J. R. Maple, M.-J. Hwang, T. P. Stockfisch, U. Dinur, M. Waldman, C. S. Ewig and A. T. Hagler, *J. Comput. Chem.*, 1994, **15**, 162.
- 57 *Discover User Guide 1995*, Biosym/Molecular Simulations Inc., San Diego, CA.